J Mol Model (2010) 16:1567–1576
DOI 10.1007/s00894-010-0678-8

ORIGINAL PAPER

Study of a structurally similar kappa opioid receptor agonist and antagonist pair by molecular dynamics simulations

Michal Kolinski · Slawomir Filipek

Received: 27 January 2010 / Accepted: 2 February 2010 / Published online: 27 February 2010

Abstract Among the structurally similar guanidinonaltrindole (GNTI) compounds, 5′-GNTI is an antagonist while 6′-GNTI is an agonist of the κOR opioid receptor. To explore how a subtle alteration of the ligand structure influences the receptor activity, we investigated two concurrent processes: the final steps of ligand binding at the receptor binding site and the initial steps of receptor activation. To trace these early activation steps, the membranous part of the receptor was built on an inactive receptor template while the extracellular loops were built using the ab initio CABS method. We used the simulated annealing procedure for ligand docking and all-atom molecular dynamics simulations to determine the immediate changes in the structure of the ligand–receptor complex. The binding of an agonist, in contrast to an antagonist, induced the breakage of the "3–7 lock" between helices TM3 and TM7. We also observed an action of the extended rotamer toggle switch which suggests that those two switches are interdependent.

Keywords GPCRs · Tight ligand pair · Receptor activation · Molecular switches · Simulated annealing · Molecular dynamics

Electronic supplementary material The online version of this article (doi:10.1007/s00894-010-0678-8) contains supplementary material, which is available to authorized users.

M. Kolinski · S. Filipek
International Institute of Molecular and Cell Biology,
4 Trojdena St,
02-109 Warsaw, Poland

S. Filipek (✉)
Faculty of Chemistry, Warsaw University,
1 Pasteur St,
02-093 Warsaw, Poland
e-mail: sfilipek@iimcb.gov.pl

Introduction

Despite many years of research, a convincing explanation for the mechanisms governing the activation of opioid receptors by typical amine ligands, opiates and their synthetic analogs is still lacking. In particular, it is not known how opioid receptors differentiate between agonists and antagonists, nor why compounds with very similar structures may exhibit opposite properties when they act on a receptor. An interesting pair of such compounds is 5′-GNTI and 6′-GNTI (Fig. 1). 5′-GTNI is a potent κOR antagonist, while 6′-GNTI is a potent agonist of the same receptor. The guanidinium group present in both compounds binds to E6.58$^{(297)}$ (numbers according to the Ballesteros–Weinstein numbering scheme [1]) on helix TM6, which leads to the large κOR selectivity of these compounds amongst opioid receptors since this amino acid is present only in κOR. Sensing mechanisms proposed so far have estimated activation effects on the basis of the structures of the complexes of the opioid receptor with docked ligands. Based on this binding mode, it was suggested by Sharma et al. [2] that the position of the guanidinium group in the agonist (6′-GNTI), in contrast with its position in the antagonist (5′-GNTI), may force the rotation of TM6, which could lead to subsequent stages of activation. However, the latest structures of activated rhodopsin (with and without a part of its G-protein, transducin [3, 4]) showed that the cytoplasmic part of TM6 moves out of the center of the receptor but that no rotation occurs, implying that the E6.58$^{(297)}$ residue stays in the same position in the receptor structure because it is located at the other end of TM6, which does not move. Another sensing/activation mechanism was proposed by Pogozheva et al. [5]. Both agonists and antagonists bind to H6.52$^{(291)}$ on TM6, but only the agonists are able to change the state of the rotamer toggle switch,

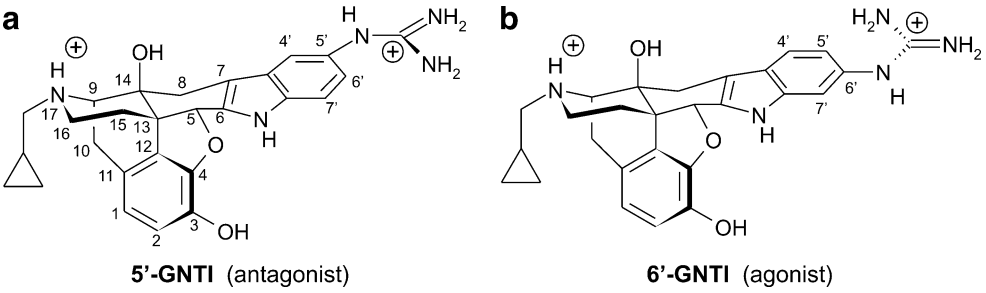

Fig. 1 Structural formulae of the antagonist 5′-GNTI (**a**) and the agonist 6′-GNTI (**b**) of κOR. Atoms are numbered for the first compound

which is suggested in this paper to be the primary activation event. However, no proof of this concept was provided. Here, based on molecular dynamics (MD) simulations of complexes of this closely related pair of compounds, we provide further support for our earlier proposition [6, 7] of a sensing/activation mechanism for opioid receptors. For the first time, using MD simulations, it was possible to explain the different properties of a structurally similar pair of ligands.

Opioid receptors belong to the A family (rhodopsin-like) of G protein-coupled receptors (GPCRs) [8–11]. There are four types of opioid receptors: δOR (OP_1), κOR (OP_2), μOR (OP_3), and the nociceptin/opioid receptor-like 1 (OP_4). Opioid receptors are involved in pain modulation and in a number of physiological functions and behavioral effects, so improving our understanding of opiate sensing, activation and signaling is of great importance, especially considering that such mechanisms may be rather general and thus also operate in other GPCRs [12]. The results may have important implications for the discovery and development of more specific medicines to treat GPCR-linked dysfunctions and diseases involving blindness, diabetes, allergies, depression, cardiovascular defects and some forms of cancer. Although GPCRs interact with a wide variety of ligands, the membranous parts of GPCRs share many similarities, since they have seven transmembrane helices linked by relatively short loops [13]. Each receptor undergoes a series of conformational rearrangements controlled by molecular switches that lead to partial or full activation, and the dynamic character of GPCRs is thought to be essential for their diverse physiological functions [14, 15].

It has been shown that GPCRs can exist as homodimers, heterodimers and higher oligomeric assemblies, and that dimerization could also play important functional roles in receptor maturation, G-protein and arrestin coupling, downstream signaling and internalization [16, 17]. Like many other GPCRs, opioid receptors undergo dimerization and may engage in cross-signaling, as shown recently for the heterodimer of the α_{2A} adrenergic receptor and μOR [18]. It was also proposed by Waldhoer et al. [19] that 6′-GNTI selectively activates opioid receptor heterodimers, δOR-κOR, but not homodimers. 6′-GNTI is an agonist of κOR but an antagonist of δOR, so there is a possibility of crosstalk between these receptors. Mechanisms of intercellular communication between GPCRs may not even require physical interaction between the receptors, as was shown for crosstalk between GABA(B) and $mGlu_{1a}$ receptors [20]. The effect of GABA(B) receptor-mediated potentiation of the mGlu receptor signaling is the result of a general mechanism in which the $G_{\beta\gamma}$ subunits produced by the G_i-coupled GABA(B) receptor enhance the mGlu-mediated G_q response. This mechanism could be also applied to other pairs of G_i- and G_q-coupled receptors. Physical interaction (dimerization) of μOR was recently shown to be nonessential for agonist and antagonist binding, and the monomeric form of μOR is a minimal functional unit capable of activating G protein [21].

Methods

Modeling unliganded opioid receptors and simulating the membrane

κOR opioid receptor structure was modeled on the basis of the crystal structure of inactive rhodopsin (Protein Data Bank code 1U19) [22]. The human κOR amino acid sequence was obtained from the Swiss-Prot database (code P41145). The structure of κOR was prepared analogously to our previous modeling of δOR and κOR [7]: the Clustal W algorithm [23] was employed to align the multiple sequences, and then manual corrections were performed to ensure that a disulfide bridge was formed by appropriate cysteine residues (multiple alignment is described in our previous paper [7]). Homology modeling was then achieved using Modeller [24, 25] and rhodopsin as a template. A single palmitoyl chain was added to cysteine 345 at the end of the cytoplasmic helix H8. Modeling the N-terminus of κOR based on rhodopsin can be a misleading approach because extracellular loops in the crystal structures of other GPCRs are markedly different, implying differences in N-termini. Therefore, the conformation of the N-terminus (residues 1–59) and the three extracellular loops (residues 121–127, 193–225 and 299–312) of κOR was predicted using an ab initio CABS method [26, 27]. In this method, sampling of the conformational space of the modeled protein takes place on a three-dimensional lattice and employs the replica

exchange Monte Carlo algorithm. The rest of the receptor structure was rigid and provided restraints for the modeled parts. A disulfide bridge (C131–C210) was also restrained to maintain a constant distance between the C_α atoms). Three κOR models with the most probable conformations were extracted from a set of 24,000 predicted structures using the HCPM clustering program [28]. Because CABS is a coarse-grain method, the modeled parts were subjected to side chain restoration and then refined by applying a simulated annealing routine implemented in GROMACS (v. 3.3) [29]. The obtained receptor models were inserted into the lipid bilayer consisting of DPPC (dipalmitoylphosphatidylcholine). The membrane containing 128 phospholipids (64 in each layer) was surrounded by water molecules in a periodic box (6.4 nm×6.4 nm×9.5 nm). The membrane had been equilibrated in an earlier simulation for 20 ns. During the insertion of the receptor into the membrane, 13 DPPC molecules were removed from the N-terminus side and 14 DPPC molecules from the C-terminus side. All minimizations and simulations were performed using GROMACS (v. 3.3). A standard FFGMX forcefield with additional parameters for lipids [30] and water SPC [31] was used to obtain a more accurate treatment of the hydrogen bonds. The PME procedure [32] was applied to treat the long-range electrostatic interactions. After energy minimization of the receptor–membrane system, three-step simulations were performed, gradually releasing the restraints. Details of the simulations and the receptor quality check after the simulations were the same as described in Kolinski et al. [7]. Simulations performed without restraints (all residues were flexible) lasted 20 ns for each of three receptor models. Because of the instability of the extracellular part of model 3 during MD simulation, we chose receptor models 1 and 2 for ligand docking and for MD simulation of complexes.

Modeling ligand–receptor complexes

The ligands were constructed in their protonated-nitrogen forms. Ligand construction and the docking procedure were analogous to those used in our earlier paper [7]. In short, the Hartree–Fock procedure employing the 6–31G* basis set in Gaussian (v.03 rev. C.02, Gaussian Inc.) was used to optimize the ligand structure, and then the RESP method [33] was applied to calculate the ligand atomic charges. The ligands were inserted into the middle of the binding pocket of κOR to preserve the interaction between D3.32$^{(138)}$ and the protonated amine nitrogens (N_{17}) of the ligands. The phenolic OH group (at carbon C_3) was initially positioned in the space between TM3 and TM6 to avoid forcing any specific location and to meet the spatial requirements of other parts of the ligands (guanidinium group). The simulated annealing procedure used to sample different binding possibilities in the binding cavity of the receptor was done as described previously [7]. This was restarted several times with the initial positions of ligands in the binding site modified manually while preserving ionic interactions between the charged amine group of a ligand and the carboxyl group of D3.32$^{(138)}$ on helix TM3, and also those between the guanidinium group and E6.58$^{(297)}$ on helix TM6. On average, about ten structures in each ligand–receptor complex were subjected to the simulated-annealing procedure. The RMSDs of the ligands at the receptor binding site after simulated annealing were not larger than 0.05 nm for all four complexes. The average structure of each complex was chosen for subsequent MD simulations. The simulated annealing procedure was performed in Yasara (v.9.10, Yasara Biosciences) with the Yamber3 forcefield (modified Amber99) at the temperature was decreased from 900 K to nearly 0 K. During this procedure, the ligand and the side chains of amino acids within a distance of 1.0 nm were allowed to move. The optimized complexes were inserted into the DPPC membrane (taken from 20 ns simulations of the empty opioid receptor in the membrane) and subjected to MD simulations. The same procedure involving the gradual release of restraints was applied, and the simulations without restraints lasted 12 ns. Representative parts of simulations of investigated complexes were converted into animations (provided as "Electronic supplementary material") in VMD software [34].

Results and discussion

Obtained receptor models

The models of κOR were generated using homology modeling techniques for transmembrane domains and the CABS method for the extracellular part of the receptor (N-terminus and loops). The template for the transmembrane part was the rhodopsin structure in its inactive state. The "ionic lock" (R3.50–E6.30) was in its "open" state in all crystallized GPCRs except for rhodopsin. In the rhodopsin structure there are both R3.50–E6.30 and R3.50–T6.34 interactions, and both of these are broken in the crystal structure of opsin. The residue T6.34 is conserved in rhodopsin and in opioid receptors (among others), but not in beta-adrenergic receptors nor in adenosine receptors (however, it is conserved in alpha-adrenergic receptors). The conservation of T6.34 in rhodopsin and opioid receptors may suggest that the cytoplasmic ends of TM3 and TM6 are in close proximity in inactive opioid receptors, similar to the rhodopsin structure. The R3.50–T6.34 interaction is preserved in our simulations, indicating that this switch is in the "closed" state in inactive opioid receptors. The rhodopsin template was used to model only the transmembrane part of the receptor, and all loops were

built using the ab initio procedure so that their structures were independent of the template.

The utilization of CABS to build the N-terminus was required to consolidate the extracellular part with transmembrane domains so as to avoid bending TM1 and moving it out of the receptor, which occurred in our earlier MD simulations of κOR and δOR models without N-termini [7]. The extracellular part of the receptor may participate in ligand binding (especially to such large ligands as 5′- and 6′-GNTI), so we used the ab initio CABS method to predict this part of the receptor structure without the influence of any templates used in homology modeling. CABS is useful for ab initio protein structure prediction, multi-template comparative modeling, and protein structure prediction based on sparse experimental data [35]. During the 6th CASP (Critical Assessment of Protein Structure Prediction) edition [36], CABS was proven to be one of the best-performing methods for protein structure prediction [37]. In order to verify the accuracy of the CABS method in modeling loops of GPCRs, we used this method to predict the conformation of the second extracellular loop, EL2 (connecting helices TM4 and TM5), in β_1- and β_2-adrenergic receptors as well as in A_{2a} adenosine receptor crystal structures, and also to predict the N-terminus structure of rhodopsin. Obtained structures exhibited low RMSD values (lower than 0.3 nm) for the predicted receptor fragments when compared to the corresponding crystal structures (Fig. 2). The EL2 loops predicted for adrenergic receptors contain helices as in crystal structures, and there is also a general similarity between the shapes of the predicted versus the crystal extracellular loops of the A_{2a} receptor. The N-terminus of rhodopsin was also modeled using CABS, and the predicted structure had a small β-sheet linked to the β-sheet of the EL2 loop, similar to the crystal structure of rhodopsin. Three models of κOR that represent the biggest clusters obtained by the CABS method and which were subjected to 20 ns MD simulations in the membrane are shown in Fig. 3. Small β-sheets are present in the N-termini of all three models of κOR. EL2 loops were also predicted by CABS to contain a β-sheet fragment, but this structure unfolded in model 1 during MD simulation. A comparison of the transmembrane segments of three models of κOR after 20 ns of MD simulation is shown in Table 1. Because of the instability of the extracellular part of model 3, we chose models 1 and 2 (the most dissimilar models) for ligand docking and MD simulations of complexes. RMSD plots for model 1 and model 2 structures are shown in Fig. 4. The transmembrane helices stabilized at the level of 0.2 nm, whereas the RMSDs calculated for all atoms reached 0.35 nm for both models of κOR. All structures stabilized after about 10 ns of simulations.

Binding modes of the agonist and the antagonist

The structures of the 6′-GNTI agonist and the 5′-GNTI antagonist are very similar. Furthermore, because of the possibility of an alternative placement of the guanidinium group, its location in space can be almost identical in both compounds (Fig. 1), ensuring similar charge distributions. Therefore, differentiating such closely related compounds

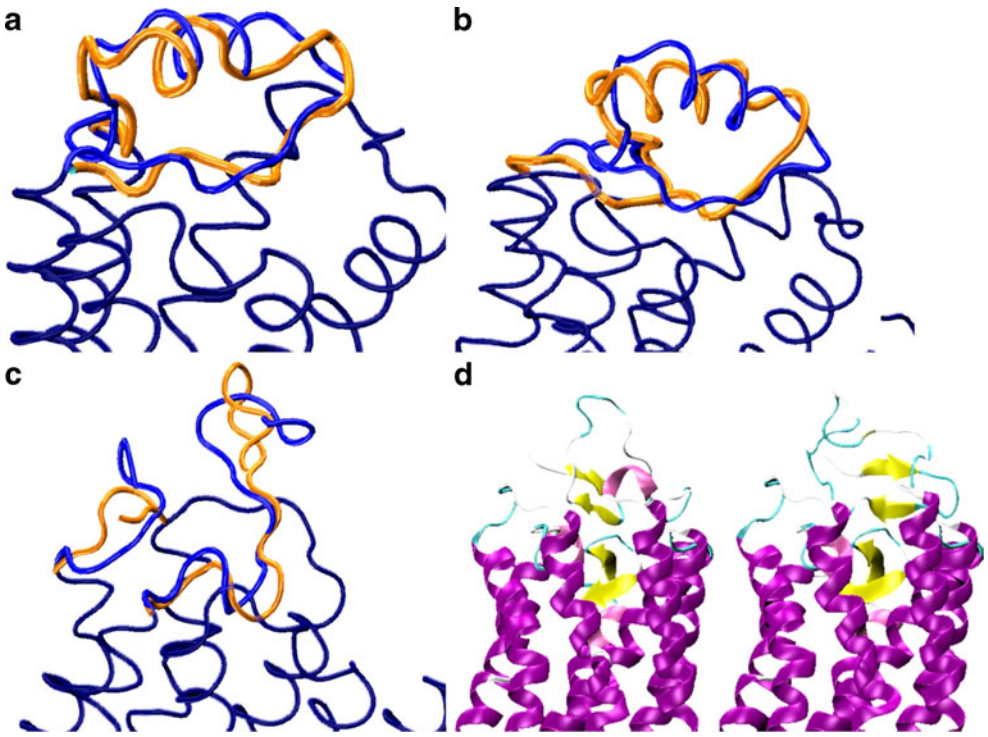

Fig. 2 Modeling the extracellular loop EL2 by the CABS method. The predicted loop is shown in *orange*. **a** β_1AR (24 amino acids), RMSD=0.20 nm. **b** β_2AR (24 amino acids), RMSD=0.26 nm. **c** A_{2a}R (31 amino acids), RMSD=0.27 nm. **d** Modeling the N-terminal part of rhodopsin (31 amino acids): crystal structure on the *left*, model on the *right*

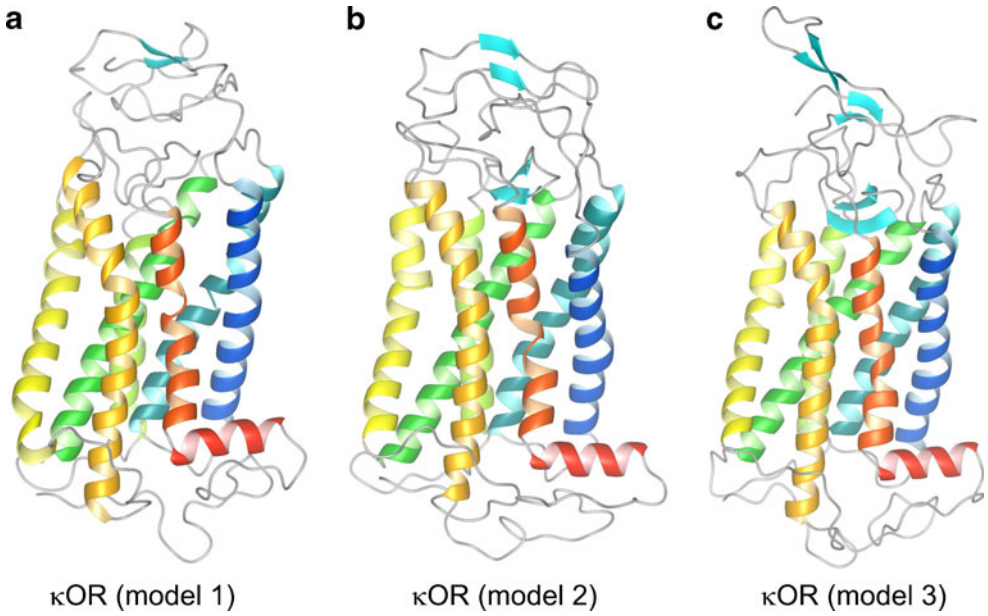

Fig. 3 The structures of κOR opioid receptor models after 20 ns of MD simulation in the membrane. They were obtained using homology modeling based on an inactive rhodopsin template and then the CABS method for modeling of extracellular parts (N-terminus and loops). **a** Model 1; **b** model 2; **c** model 3. Transmembrane helices are colored according to a rainbow color scheme: TM1 in *blue*, TM2 in *light blue*, TM3 in *green*, TM4 in *yellow-green*, TM5 in *yellow*, TM6 in *orange*, and TM7 in *red*

by the receptor could be a tricky task. The binding modes of 5′- and 6′-GNTI obtained using the simulating annealing procedure were similar to those discovered in our earlier studies for tyramine-based ligands of the three opioid receptors δOR, κOR and μOR [6, 7] (antagonists: naltrexone, naltrindole, norBNI, β-FNA; agonists: morphine, N-methyl-morphine and butorphanol). One of the antagonists, norBNI, contains two charged amine groups. The GNTI compounds also possess two charged groups, providing natural restraints on binding to the receptor. There are experimentally well-documented ionic interactions of both charged functional groups, namely that of the protonated nitrogen N_{17} with D3.32$^{(138)}$ and that of the guanidinium group with E6.58$^{(297)}$. Such interaction sites form a vertical axis. We found that the phenolic hydroxyl group of the antagonist 5′-GNTI was bound to Y3.33$^{(139)}$ (Fig. 5), whereas that of the agonist was bound to H6.52$^{(291)}$ (Fig. 6). Movement between these residues is horizontal and does not violate ionic restraints. The localization of the guanidinium group of the antagonist was markedly different in each κOR model because it was located on alternative sides of E6.58$^{(297)}$ (Fig. 5), but even so, the binding of the antagonist to Y3.33$^{(139)}$ prevented the receptor from performing any activation activities, as can be seen from the monitored distances (especially that of the 3–7 lock switch, which is a hydrogen bond, D3.32$^{(138)}$–Y7.43$^{(320)}$, between helices TM3 and TM7), which stayed the same during the whole simulation. However, after the rotation of a ligand at the binding site and the creation of a bond with H6.52$^{(291)}$, the 3–7 lock broke in both models of κOR. In model 1 this breakage took over 5 ns, whereas in model 2 it happened in a single event after about 2.5 ns of simulation. At the beginning of the MD simulation of model 2, the agonist was bound to both Y3.33$^{(139)}$ and H6.52$^{(291)}$, and during the first nanosecond of simulation the bond to histidine was broken, so the agonist adopted an antagonist binding mode. After 1 ns, 6′-GNTI restored its firm binding to H6.52$^{(291)}$, but the bond to Y3.33$^{(139)}$ was restored several times. This did not, however, influence the broken 3–7 lock (Fig. 6b). A quantitative description of the occupancies of particular hydrogen bonds during 12 ns MD simulations of complexes

Table 1 A comparison of the transmembrane (TM) segments of three models of κOR after 20 ns of molecular dynamics simulation

κOR RMSD (nm)	$TM_{backbone}$	$TM_{all\ atoms}$
model 1 − model 2	0.215	0.287
model 1 − model 3	0.181	0.254
model 2 − model 3	0.144	0.226

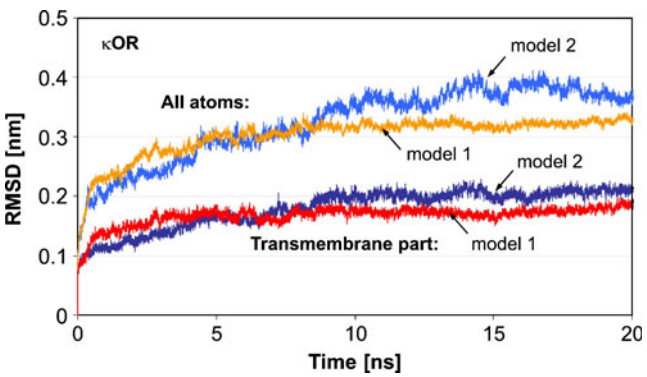

Fig. 4 Root mean square displacement (RMSD) plots for unconstrained 20 ns MD simulations of unliganded model 1 and model 2 of κOR in the membrane. The *two lower curves* show the RMSDs of transmembrane helices only, and the *two upper curves* take into account all atoms

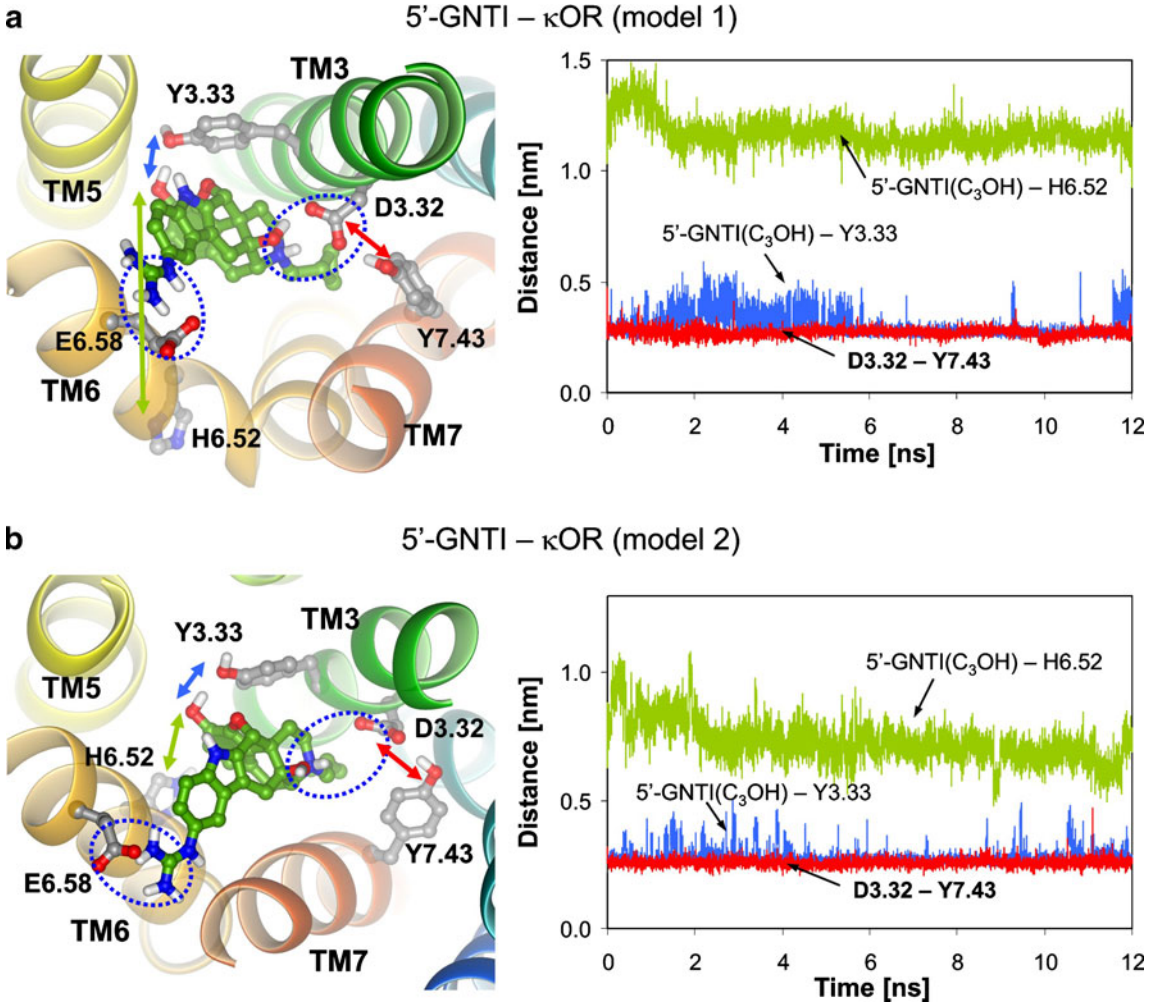

Fig. 5 The binding modes of the antagonist 5′-GNTI and plots of selected distances within the binding sites of model 1 (**a**) and model 2 (**b**) of κOR. View from the extracellular side. Distances (in structures and plots): D3.32$^{(138)}$–Y7.43$^{(320)}$ 3–7 lock in *red*, ligand(C_3OH)–Y3.33$^{(139)}$ in *blue*, and ligand(C_3OH)–H6.52$^{(291)}$ in *green*. *Dashed ellipses* denote ligand–receptor ionic interactions

with the agonist and the antagonist is provided in Table 2. An additional Y7.35$^{(312)}$–guanidinium group interaction was found only in receptor–agonist complexes, but its low occupancy in the κOR model 1 agonist case may suggest that such a link is nonspecific. The representative parts of the molecular dynamics simulations of complexes of 5′-GNTI and 6′-GNTI with models 1 and 2 of κOR are shown in animations (see Animations 1, 2, 3, 4 in the "Electronic supplementary material").

Activation events evoked by the agonist

The question then arises as to whether the horizontal movement of a ligand between TM3 and TM6 (i.e., from Y3.33$^{(139)}$ to H6.52$^{(291)}$) alone, regardless of the structure of the ligand, is enough to evoke activation changes in the receptor. We answered this question in our earlier studies using naltrexone, which is a nonselective antagonist of all three opioid receptors. Its binding to Y3.33$^{(139)}$ was stable and it did not perturb the receptor, but when it was forced to bind H6.52$^{(291)}$, while the ionic interaction with D3.32$^{(138)}$ preserved, the 3–7 lock was broken in all three receptor models: δOR, κOR and μOR. To study the final movements of the ligand at the receptor binding site and the resulting immediate changes in the receptor structure of κOR, it was necessary to use the template of an inactive receptor. The configurations of the switches in crystallized receptors other than rhodopsin (β_1AR, β_2AR and A_{2a}R) suggest that some activation steps (evoked either by the introduction of lysozyme or by a bound inverse agonist) have already occurred. Based on virtual screening results [38] and also on data from a MD simulation of β_2AR [39], it was postulated that the docking of agonists such as epinephrine (which is smaller than the ligand in the crystal structure) requires changes in the positions of transmembrane helices, resulting in the shrinkage of the binding site. The usage of rhodopsin instead of crystal structures of other GPCRs may cause some reservations because of the tight

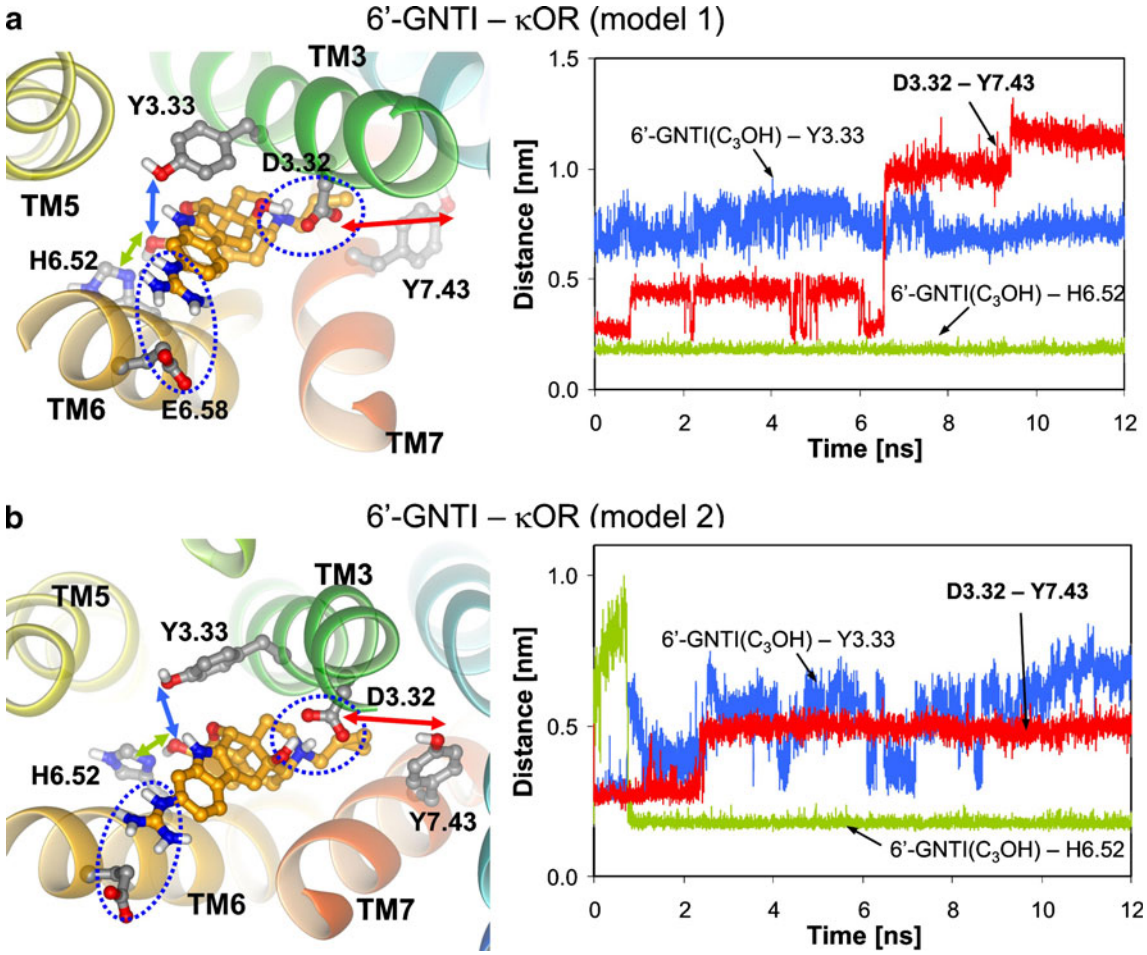

Fig. 6 The action of agonist 6′-GNTI, its binding mode, and plots of selected distances within the binding sites of model 1 (**a**) and model 2 (**b**) of κOR. *Colors of distances* are the same as in Fig. 5

EL2 loop penetrating deeply into the binding site. However, the CABS method was used to predict the structure of this loop, and also, during the simulated annealing procedure used to elucidate the ligand binding and tweak the receptor structure, it was found that this loop was moved toward the extracellular part of the receptor in both models of κOR, and it was finally located at a position similar to that in the A_{2a} receptor. Such a position and conformation of EL2 allow diffusional motions of ligands to and from the receptor. Furthermore, both GNTI ligands were bound to the binding site of κOR at a position similar to that of an inverse agonist (Fig. 7) in the crystal structure of $A_{2a}R$ (3EML code in the Protein Data Bank) [40].

The central switch investigated in this paper, which involves breaking the connection between TM3 and TM7, was proposed for rhodopsin by the Khorana group [41], based on mutagenesis experiments. According to their findings, the salt bridge E113–K296 (E3.28–K7.43) linking helices TM3 and TM7 is a key constraint that maintains the resting state of the receptor. The authors demonstrated that the K296–E113 connection may be a switch that, when broken through mutagenesis, results in a movement of TM6

Table 2 Occupancies of the 3–7 lock and receptor–ligand hydrogen bonds during 12 ns of MD simulations of complexes with the agonist and the antagonist

Interactions / occupancies (%)	$D3.32^{(138)}$–$Y7.43^{(320)}$	$Y3.33^{(139)}$–$C_{(3)}OH$	$H6.52^{(291)}$–$C_{(3)}OH$	$Y7.35^{(312)}$– guanidinium group
κOR model 1 − agonist	12.0	0	100	20.3
κOR model 2 − agonist	17.2	10.1	93.7	91.6
κOR model 1 − antagonist	92.9	75.7	0	0
κOR model 2 − antagonist	99.1	93.9	0	0

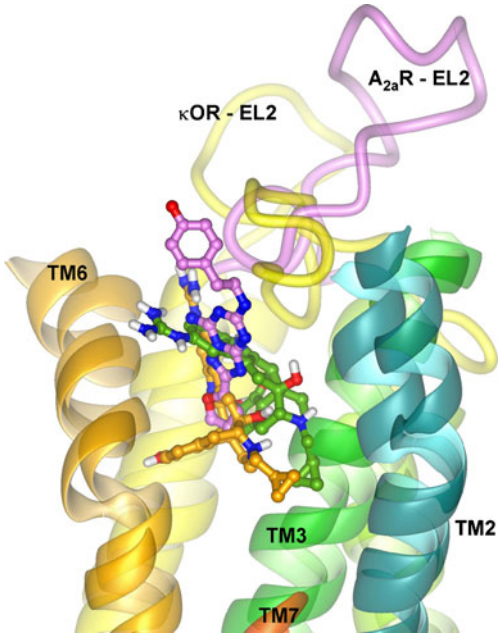

Fig. 7 Superposition of the κOR–agonist (carbon atoms in *orange*) and κOR–antagonist (carbon atoms in *green*) models and the crystal structure of $A_{2a}R$ with the inverse agonist (carbon atoms in *violet*). To make the picture clearer, some of the helices and loops were removed

that is similar but not identical to that caused by photoactivation of the WT receptor. Another switch involving a connection between TM3 and TM6 in κOR is established by R3.50 and T6.34. There is no E6.30 residue in TM6 of κOR that can form a salt bridge with R3.50, unlike in rhodopsin and other crystal structures of GPCRs. The residue T6.34 also exists in rhodopsin and forms an additional hydrogen bond with R3.50, so TM3 and TM6 form a stronger link. In our simulations of κOR complexes, the R3.50–T6.34 connection stayed unbroken for both agonists and antagonists, following our earlier results obtained for μOR [6]. The stability of the TM3–TM6 link is consistent with the initial steps of receptor activation that our investigations were confined to.

Possible coupling of two switches

In a similar manner to our earlier studies, we have also seen concerted motions of W6.48$^{(287)}$ and H6.52$^{(291)}$, which are located on the same face of helix TM6. They constitute an extended rotamer toggle switch based on the motif CWx$P_{6.50}$xF/H. The χ_1 and χ_2 angles of both residues during the simulation of the 6'-GNTI-κOR complex (model 2) are shown in Fig. 8. During the first nanosecond of simulation, the ligand detached from TM6 (Fig. 6) and stayed temporarily bound to TM3 in an antagonist binding mode. This binding evoked a change of rotamers of W6.48$^{(287)}$ and H6.52$^{(291)}$ to match the antagonist binding mode. The successive change in rotamers to positions suited to the agonist binding mode occurred after 10 ns, 8 ns after the 3–7 lock was broken. Also, in this case the change in the histidine rotamer followed that of tryptophan, which means that the change in the W6.48$^{(287)}$ side chain initiates the extended rotamer toggle switch. No such action of the rotamer toggle switch was observed for model 1 because of the earlier usage of a simulated annealing procedure that set the rotamers in an agonist binding mode.

The nanosecond timescale used in the simulations conducted here is small compared to the milliseconds required for full activation of the receptor. However, we only investigated events concurrent to ligand binding, and the ligands were already placed at the binding site (with the help of a simulated annealing procedure confined to a small area of the receptor), so the usage of such a timescale is justified. Changes in protein structure involving large structural rearrangements are usually slow, but the motions of individual amino acids, especially those involving bond breaking or creation or conformational changes in amino acid side chains (such motions constitute the actions of switches), are rather fast and can be tracked down by molecular dynamics simulations employing a nanosecond timescale. The actions of switches are then followed by large and much slower rearrangements of protein structure. In 12 ns MD simulations of both κOR models, the agonist

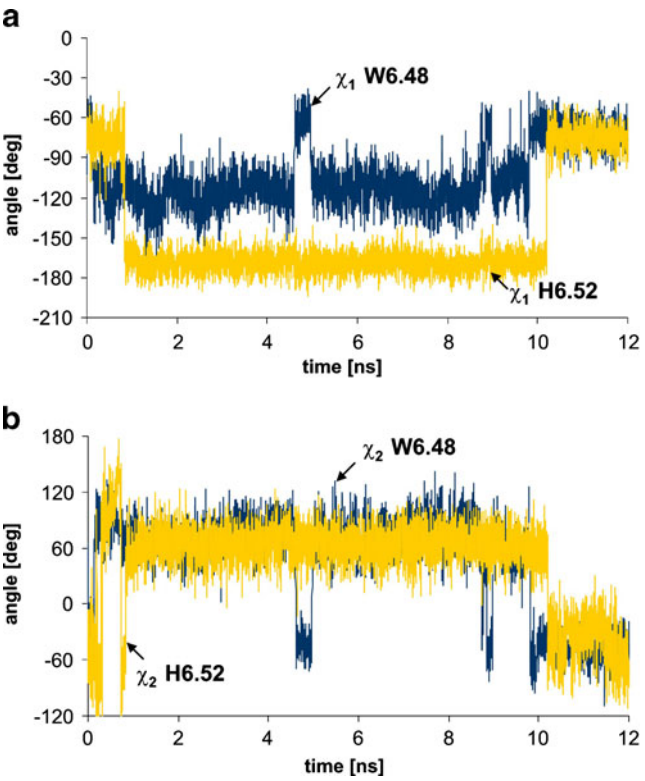

Fig. 8 Plots from the 12 ns MD simulation of the κOR–agonist complex (model 2) showing the χ_1 (**a**) and χ_2 (**b**) angles of the W6.48$^{(287)}$ and H6.52$^{(291)}$ residues, illustrating the extended rotamer toggle switch (based on the motif CWxPxF/H)

6'-GNTI yielded complete breakage of the 3–7 lock while the bond to Y3.33$^{(139)}$ was not restored (Fig. 6) fast enough to stop other changes in receptor structure and especially the extended rotamer toggle switch from occurring. Because the time span between these events is very small (nanoseconds) compared to the time needed for full receptor activation (milliseconds), both switches may be coupled.

Residues D3.32 and Y7.43 (which form the 3–7 lock in opioid receptors) are well conserved among GPCRs, especially in amine class receptors (they occur in 88% of such receptors, including alpha- and beta- adrenoceptors, serotonin, muscarinic, dopamine, and partly histamine receptors) and peptide class receptors (10%, including opioid, urotensin II and somatostatin receptors). The pair Y3.33 and H6.52 seems to be specific to opioid receptors (it also exists in a few GPCRs, like viral and purinoceptors). Nevertheless, other residues in these or adjacent locations can serve as anchor points to differentiate agonists and antagonists. However, simple conservation of these residues does not guarantee preservation of the mechanism. A possible switch, D3.32–Y7.43, in beta-adrenergic receptors is modified by N7.39 nearby, which is present neither in opioid receptors nor in rhodopsin. On the other hand, the 3–7 lock exists in a modified form (E3.28–K7.43) in rhodopsin. The pair W6.48 and H6.52 exist in 24% of the peptide class of GPCRs, but H6.52 can be easily replaced with other residues like tyrosine (10% in the peptide class) or phenylalanine (24% in the peptide class, 76% in the amine class), and they will perform the same concerted movements in the rotamer toggle switch.

Conclusions

The observed binding modes for the structurally similar agonist–antagonist pair and the scenario for the early activation steps confirm our earlier findings for μOR, δOR and κOR opioid receptors. The current results were obtained for two different models of κOR with docking performed independently, so the positions of the same ligands were different although the distinctive features of agonist versus antagonist binding were preserved: the antagonist was bound with its tyramine group to Y3.33$^{(139)}$ on helix TM3, while the antagonist was bound to H6.52$^{(291)}$ on helix TM6. In all cases the guanidinium group was bound to E6.58$^{(297)}$ on helix TM6. Activation events, 3–7 lock (between helices TM3 and TM7) breaking and extended rotamer toggle switch action, were evoked only in the case of the agonist 6′-GNTI, despite the similarity in the shapes and electrostatic properties of 6′-GNTI and 5′-GNTI. To make it possible to differentiate such a closely related ligand pair, the sensing mechanism at the binding site of the receptor must operate in an extremely confined area, like that proposed by us. Our studies were conducted on monomeric receptor structures, and it was recently shown for μOR that the monomer is the minimal unit needed to bind ligands and activate G protein. However, dimerization may additionally modify receptor–ligand interactions as well as activation routes, making cross-talk between GPCRs exceptionally complicated. Elucidating the mechanisms of ligand binding and the early activation steps may lead to a better understanding of the onset of signaling processes and also to more efficient drug design.

Acknowledgments The work was supported by the Polish Ministry of Science and Higher Education (Grant no. N N301 2038 33). M. Kolinski acknowledges the School of Molecular Medicine for a stipend that supported his Ph.D. study.

References

1. Ballesteros JA, Weinstein H (1995) Integrated methods for the construction of three-dimensional models and computational probing of structure-function relations in G protein-coupled receptors. Methods Neurosci 25:366–428
2. Sharma SK, Jones RM, Metzger TG, Ferguson DM, Portoghese PS (2001) Transformation of a kappa-opioid receptor antagonist to a kappa-agonist by transfer of a guanidinium group from the 5′- to 6′-position of naltrindole. J Med Chem 44:2073–2079. doi:10.1021/jm010095v
3. Scheerer P, Park JH, Hildebrand PW, Kim YJ, Krauss N, Choe HW, Hofmann KP, Ernst OP (2008) Crystal structure of opsin in its G-protein-interacting conformation. Nature 455:497–502. doi:10.1038/nature07330
4. Park JH, Scheerer P, Hofmann KP, Choe HW, Ernst OP (2008) Crystal structure of the ligand-free G-protein-coupled receptor opsin. Nature 454:183–188. doi:10.1038/nature07063
5. Pogozheva ID, Przydzial MJ, Mosberg HI (2005) Homology modeling of opioid receptor-ligand complexes using experimental constraints. AAPS J 7:E434–E448. doi:10.1208/aapsj070243
6. Kolinski M, Filipek S (2008) Molecular dynamics of mu opioid receptor complexes with agonists and antagonists. TOSBJ 2:8–20. doi:10.2174/1874199100802010008
7. Kolinski M, Filipek S (2009) Studies of the activation steps concurrent to ligand binding in DOR and KOR opioid receptors based on molecular dynamics simulations. TOSBJ 3:51–63. doi:10.2174/1874199100903010051
8. Dreborg S, Sundstrom G, Larsson TA, Larhammar D (2008) Evolution of vertebrate opioid receptors. Proc Natl Acad Sci USA 105:15487–15492. doi:10.1073/pnas.0805590105
9. Waldhoer M, Bartlett SE, Whistler JL (2004) Opioid receptors. Annu Rev Biochem 73:953–990. doi:10.1146/annurev.biochem.73.011303.073940
10. Corbett AD, Henderson G, McKnight AT, Paterson SJ (2006) 75 years of opioid research: the exciting but vain quest for the Holy Grail. Br J Pharmacol 147:S153–S162. doi:10.1038/sj.bjp.0706435
11. Kane BE, Svensson B, Ferguson DM (2006) Molecular recognition of opioid receptor ligands. AAPS J 8:E126–E137. doi:10.1208/aapsj080115
12. Strange PG (2008) Signaling mechanisms of GPCR ligands. Curr Opin Drug Discov Dev 11:196–202
13. Mirzadegan T, Benko G, Filipek S, Palczewski K (2003) Sequence analyses of G-protein-coupled receptors: similarities to rhodopsin. Biochemistry 42:2759–2767. doi:10.1021/bi027224+

14. Kobilka BK, Deupi X (2007) Conformational complexity of G-protein-coupled receptors. Trends Pharmacol Sci 28:397–406. doi:10.1016/j.tips.2007.06.003
15. Kobilka BK (2007) G protein coupled receptor structure and activation. Biochim Biophys Acta Biomembr 1768:794–807. doi:10.1016/j.bbamem.2006.10.021
16. Terrillon S, Bouvier M (2004) Roles of G-protein-coupled receptor dimerization—from ontogeny to signalling regulation. EMBO Rep 5:30–34. doi:10.1038/sj.embor.7400052
17. Milligan G (2008) A day in the life of a G protein-coupled receptor: the contribution to function of G protein-coupled receptor dimerization. Br J Pharmacol 153:S216–S229. doi:10.1038/sj.bjp.0707490
18. Vilardaga JP, Nikolaev VO, Lorenz K, Ferrandon S, Zhuang Z, Lohse MJ (2008) Conformational cross-talk between alpha2A-adrenergic and mu-opioid receptors controls cell signaling. Nat Chem Biol 4:126–131. doi:10.1038/nchembio.64
19. Waldhoer M, Fong J, Jones RM, Lunzer MM, Sharma SK, Kostenis E, Portoghese PS, Whistler JL (2005) A heterodimer-selective agonist shows in vivo relevance of G protein-coupled receptor dimers. Proc Natl Acad Sci USA 102:9050–9055. doi:10.1073/pnas.0501112102
20. Rives ML, Vol C, Fukazawa Y, Tinel N, Trinquet E, Ayoub MA, Shigemoto R, Pin JP, Prezeau L (2009) Crosstalk between GABA (B) and mGlu1a receptors reveals new insight into GPCR signal integration. EMBO J 28:2195–2208. doi:10.1038/emboj.2009.177
21. Kuszak AJ, Pitchiaya S, Anand JP, Mosberg HI, Walter NG, Sunahara RK (2009) Purification and functional reconstitution of monomeric mu-opioid receptors. Allosteric modulation of agonist binding by Gi2. J Biol Chem 284:26732–26741. doi:10.1074/jbc.M109.026922
22. Okada T, Sugihara M, Bondar AN, Elstner M, Entel P, Buss V (2004) The retinal conformation and its environment in rhodopsin in light of a new 2.2 angstrom crystal structure. J Mol Biol 342:571–583. doi:10.1016/j.jmb.2004.07.044
23. Thompson JD, Higgins DG, Gibson TJ (1994) CLUSTAL W: improving the sensitivity of progressive multiple sequence alignment through sequence weighting, position-specific gap penalties and weight matrix choice. Nucleic Acids Res 22:4673–4680
24. Sali A, Potterton L, Yuan F, van Vlijmen H, Karplus M (1995) Evaluation of comparative protein structure modeling by MODELLER. Proteins 23:318–326. doi:10.1002/prot.340230306
25. Sanchez R, Sali A (1997) Evaluation of comparative protein structure modeling by MODELLER-3. Proteins Suppl 1:50–58
26. Kolinski A, Skolnick J (2004) Reduced models of proteins and their applications. Polymer 45:511–524
27. Kolinski A (2004) Protein modeling and structure prediction with a reduced representation. Acta Biochim Pol 51:349–371
28. Gront D, Hansmann UHE, Kolinski A (2005) Exploring protein energy landscapes with hierarchical clustering. Int J Quantum Chem 105:826–830. doi:10.1002/qua.20741
29. Van der Spoel D, Lindahl E, Hess B, Groenhof G, Mark AE, Berendsen HJC (2005) GROMACS: fast, flexible, and free. J Comput Chem 26:1701–1718. doi:10.1002/jcc.20291
30. Berger O, Edholm O, Jahnig F (1997) Molecular dynamics simulations of a fluid bilayer of dipalmitoylphosphatidylcholine at full hydration, constant pressure, and constant temperature. Biophys J 72:2002–2013. doi:10.1016/S0006-3495(97)78845-3
31. van der Spoel D, van Maaren PJ, Berendsen HJC (1998) A systematic study of water models for molecular simulation: derivation of water models optimized for use with a reaction field. J Chem Phys 108:10220–10230. doi:10.1063/1.476482
32. Darden T, York D, Pedersen L (1993) Particle mesh Ewald: An N·log(N) method for Ewald sums in large systems. J Chem Phys 98:10089–10092. doi:10.1063/1.464397
33. Bayly CI, Cieplak P, Cornell WD, Kollman PA (1993) A well-behaved electrostatic potential based method using charge restraints for deriving atom-centered charges: the RESP model. J Phys Chem 97:10269–10280. doi:10.1021/j100142a004
34. Humphrey W, Dalke A, Schulten K (1996) VMD: visual molecular dynamics. J Mol Graph 14:33–38
35. Latek D, Ekonomiuk D, Kolinski A (2007) Protein structure prediction: combining de novo modeling with sparse experimental data. J Comput Chem 28:1668–1676. doi:10.1002/jcc.20657
36. Moult J (2005) A decade of CASP: progress, bottlenecks and prognosis in protein structure prediction. Curr Opin Struct Biol 15:285–289. doi:10.1016/j.sbi.2005.05.011
37. Kolinski A, Bujnicki JM (2005) Generalized protein structure prediction based on combination of fold-recognition with de novo folding and evaluation of models. Proteins 61(Suppl 7):84–90
38. Reynolds KA, Katritch V, Abagyan R (2009) Identifying conformational changes of the beta(2) adrenoceptor that enable accurate prediction of ligand/receptor interactions and screening for GPCR modulators. J Comput Aided Mol Des 23:273–288. doi:10.1007/s10822-008-9257-9
39. Huber T, Menon S, Sakmar TP (2008) Structural basis for ligand binding and specificity in adrenergic receptors: implications for GPCR-targeted drug discovery. Biochemistry 47:11013–11023. doi:10.1021/bi800891r
40. Jaakola VP, Griffith MT, Hanson MA, Cherezov V, Chien EYT, Lane JR, Ijzerman AP, Stevens RC (2008) The 2.6 angstrom crystal structure of a human A(2A) adenosine receptor bound to an antagonist. Science 322:1211–1217. doi:10.1126/science.1164772
41. Kim JM, Altenbach C, Kono M, Oprian DD, Hubbell WL, Khorana HG (2004) Structural origins of constitutive activation in rhodopsin: role of the K296/E113 salt bridge. Proc Natl Acad Sci USA 101:12508–12513. doi:10.1073/pnas.0404519101